UWB Radar with Array Antennas for Human Respiration and Heartbeat Detection

Huan-Bang Li and Ryu Miura
Dependable Wireless Network Laboratory
Natioanl Institite of Information and Communications Technology (NICT)
Yokosuka, Japan
{lee, Ryu}@nict.go.jp

***Abstract*— Detection of human respiration and heartbeat is an essential demand in medical monitoring, healthcare vigilance, as well as in rescue activities. Radar is an important tool to detect human respiration and heartbeat. Compared to body-attached sensors, radar has the advantage of detection without contact to a subject, which is favorable in practical usage. We conducted preliminary studies on ultra-wideband (UWB) radar for detection of respiration and heartbeat by computer simulations in this paper. The main achievement of our work is the development of a UWB radar simulation system, which is designed in line with real implementation. Using the developed system, three UWB frequency bands are compared for respiration and heartbeat detection. The effects of using antenna arrays are also examined.**

Keywords- UWB radar; antenna array; respiration detection; heartbeat detection; UWB bands

I. INTRODUCTION

Detection of human respiration and heartbeat is of essential importance in medical and healthcare services. Some examples are patient's status tracking in medical triage, routine monitoring in elderly healthcare, searching of survivals under rubble of earthquake aftermath, and so on. Although respiration and heartbeat can be obtained by using body-attached sensors, detection without physical intervention to human body is much more comfort and convenient in practical usage. Radar is an important tool to detect human respiration and heartbeat without physical intervention to a subject. Researchers have been conducting studies on respiration and heartbeat detecting radars for decades. Some recent works can be found in [1-5, 8].

Doppler radar is often used for respiration and heartbeat detection [1-3]. In this case, the Doppler shift incurred by respiratory and circulatory contraction and expansion is measured by a continuous wave (CW) radar. Generally, the reflections and interference of surrounding scatters as well as interference between the respiration and heartbeat degrade the detection sensitivity. Using higher frequency is helpful to increase the detection sensitivity. L. Chioukh, et al. evaluated the effects of frequencies for 5.8 GHz, 24 GHz, and 35 GHz, and concluded that the highest sensitivity detection is achieved at the highest frequency [1].

UWB radar for human tracking had been studied by several researchers [6-7]. Moreover, many authors had conducted studies on respiration and heartbeat detection using UWB radars. In [4], a pulse generator at the transmitter and a sampler at the receiver were used to detect respiration using UWB pulses at 0.5GHz - 2.5GHz. In [5], design issues for UWB radar at 3.1-10.6 GHz with 90nm CMOS were discussed.

In this paper, we present preliminary results of UWB radars for detection of respiration and heartbeat by computer simulations. We developed a computer simulation system for UWB radar in line with real implementation. UWB bands are different in countries and regions, the developed radar simulation system mainly targets at the frequency bands that are allowed in Japan, while with the frequency band allowed in USA as comparison. Moreover, antenna array models are developed to investigate the effects of the number of antennas under the constraint of maximum total radiation limits.

The rest of the paper is organized as follows. In section II, the developed simulation system of UWB radar and the detection principle are illustrated in detail. In Section III, the simulation setting and models are described. Then, examples of simulation results and discussions are presented in section IV. A short conclusion of the paper is given in Section V.

II. SYSTEM OVERVIEW

The block diagram of the developed UWB radar system for simulation is shown in Figure 1. The clock generator generates strobe pulses with a frequency of f_{cg} for synchronization of all modules in the system. In pseudo random (PN) dither module, strobe pulses are randomized in accordance with PN M-sequence. Each strobe pulse triggers a random PN number according to the law of M-sequence. Period of M-sequence in time unit is given by

$$T_{PN} = \frac{N_{PN}}{f_{cg}} \tag{1}$$

where, N_{PN} denotes the length of the M-sequence. Each strobe pulse arrived at PN dither will be delayed by a time interval that is linearly related to the PN numbers. The maximum delay corresponds to the maximum number of M-sequence and it does not exceed the period of strobe pulse.

 ISBN: 978-1-61208-306-3

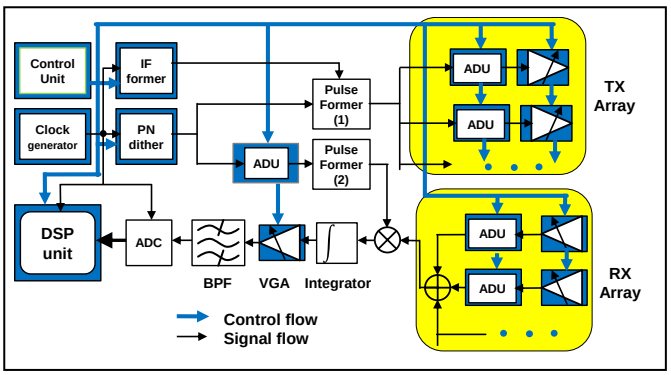

Figure 1. Block diagram of the UWB radar simulation system.

There are two main purposes to perform pulse randomization. Firstly, randomization can reduce the line spectrum components at frequencies that are multiples of clock frequency f_{cg}. Secondly, randomization makes the signal spectrum more noise-like, which is favourable for better electromagnetic compatibility and for achieving efficient usage of power spectral density. Finally, the PN dither outputs randomized pulse sequence, whose repetition period is equal to T_{PN}.

After PN dither, the randomized pulse sequence is divided into two equivalent parts. On one hand, the first part is sent to pulse former (1) to generate UWB pulse for emission. On the other hand, the second part is passed through a variable delay module and sent to pulse former (2) to generate a heterodyne signal for signal detection at the receiver. At pulse former (1), randomized pulse sequence is modulated by an IF former. The latter operates on the clock frequency f_{cg} and generates periodic square signal with a period of $2 \times T_{PN}$. Therefore, pulse former (1) is switched on during the first T_{PN} interval and outputs the randomized pulse sequence. Pulse former (1) is switched off during the second T_{PN} interval without outputs. Another role of the IF former is that it enables the use of bandpass amplifier working at intermediate frequency at receiver. That eliminates the flicker noise in the amplification of the received signals. In contrast, pulse former (2) outputs a delayed version of randomized pulse sequence continuously.

Pulse burst from pulse former (1) is sent to the transmit antenna array (TX array). At TX array, input signal is divided and fed into every element. Each element of the TX array contains an adjustable delay unit (ADU), a variable gain amplifier (VGA), and an antenna. The ADUs can be used to coordinate delays among antennas. After delay and amplification, UWB pulses are emitted towards subject. The numbers of array antennas enabled in the simulation system are 1×1, 2×2, and 4×4, respectively.

The emitted UWB signal is reflected by the subject. A sequence of reflected pulses is received by the receive antenna array (Rx array). Each element of the RX array contains an antenna, a VGA, and an ADU. ADUs are used to coordinate delays among receiving antennas. The received signals from all elements are added and fed into the mixer, where the received signal is demodulated using the heterodyne signal from pulse former (2). The output of the Mixer is passed to the integrator.

If the received signal matches with the heterodyne signal, the integrator outputs correlated signal, which strength is proportional to the amplitude of the received signal with the period of $2 \times T_{PN}$. By taking advantage of the huge bandwidth of UWB, we use a range-gated architecture with a basic sensing resolution element of dR.

$$dR = \frac{d_t \times c}{2} \quad (2)$$

where c is speed of light and d_t is the UWB pulse length measured at -10 dB level. The latter varies in accordance with frequencies and bandwidths. We can detect a number of N_{dR} resolution elements by sequentially sending N_{dR} of pulse bursts and adjusting variable delay for pulse former 2, so that each pulse burst corresponds to one out of the N_{dR} elements.

Then, the signal is amplified by VGA to compensate signal attenuation due to reflection and transmission. Finally, the signal is filtered by BPF and passed through analogue digital converter (ADC) and then fed into the digital signal processing (DSP) unit. The sampling frequency is same as the clock frequency f_{cg}.

The structure of DSP is shown in Figure 2. In amplitude detector module, the input signal is divided into in-phase and quadrature-phase components and converted into baseband signal. Square root samples of envelope of the baseband signal are calculated for each resolution element. The obtained envelope samples are sent to the bin decimation module, where decimation is performed while keeping the resulted sampling frequency large enough to recover the targeting objective.

The signal reflected from stationary objects, repeats in each sweep and presents as DC component in each resolution element. Infinite impulse response (IIR) filter of the first order is applied as Bin DC filter to remove the DC component and to output realizations of samples. In the cyclic buffer module, a number of N_{FFT} counts of realizations are stored for each of the N_{dR} resolution element.

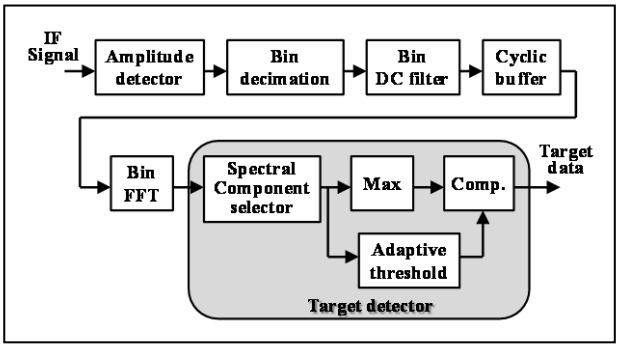

Figure 2. Structure of DSP unit.

When the buffer is full of N_{FFT} counts, a new incoming count will drive out the oldest count so that the buffer is continuously updated. Then, Bin FFT module performs sequentially moving fast Fourier transform (FFT) with pre-weighting by windowing function. A weighted realization can be written as

$$S_{bin\_win\_i}(n) = S_{bin\_i}(n) \times win(n); \quad n = 0,\ 1,\ \cdots,\ N_{FFT} - 1 \tag{3}$$

where $S_{bin\_i}(n)$ denotes the n'th realization of N_{FFT} counts for *i*th resolution element, and *win*(*n*) denotes the weighting window. Bin FFT is performed as follows.

$$\dot{S}_{bin\_FFT\_i}(k) = \sum_{n=0}^{N_{FFT}-1} S_{bin\_win\_i}(n) \cdot \exp\left(-i \cdot \frac{2\pi}{N_{FFT} - 1} \cdot n \cdot k\right); \quad k = 0,\ 1,\ \cdots,\ N_{FFT} - 1. \tag{4}$$

The resulted spectral sample is given by

$$\left|\dot{S}_{bin\_FFT\_i}(k)\right| = \sqrt{\mathrm{Re}\left(\dot{S}_{bin\_FFT\_i}(k)\right)^2 + \mathrm{Im}\left(\dot{S}_{bin\_FFT\_i}(k)\right)^2} \tag{5}$$

Finally, the resulted spectral samples are sent to target detectors. In which, corresponding spectral components of respiration and heartbeat are tuned. The maximum value is chosen from the tuned spectral components, which is compared with a threshold. If the spectral component is larger than the threshold, the corresponding subject is detected.

III. SIMULATION SETTING

In this section, we describe the assumptions and conditions that are used to carry out simulations with the developed UWB radar system. We first show the frequency bands examined, which affect the UWB pulses directly. Then, parameters related to radar as well as parameters of subject to be detected are illustrated.

A. Frequency Bands

The available UWB bands are different in countries or regions. In the developed simulation system, we mainly investigate the following three frequency bands.

(1) 3.4 - 4.8 GHz
(2) 7.25 – 10.25 GHz
(3) 3.1 -10.6 GHz

where, (1) and (2) are UWB low band and high band regulated in Japan, while (3) is UWB band regulated in USA. The reason that we select both low band and high band of Japan is that low band will be impelled to more strict regulation, although low frequency is suitable for radar in general. A UWB pulse can be expressed as

$$s(t) = A_{\max} \exp\left(-a^2 t^2\right) \sin\left(2\pi f_c t - \pi\right) \tag{6}$$

where, f_c is the center frequency of the corresponding band, a is a pulse parameter and is dependent on UWB band. A_{max} is the maximum amplitude, which is restricted by regulations and is also dependent on UWB band. For the above three UWB bands and different antenna arrays, these parameters are summarized in Table I.

TABLE I. PULES PARAMETERS RELATED TO UWB BANDS

Parameter		**3.4-4.8GHz**	**7.25-10.25GHz**	**3.1-10.6GHz**
Central frequency f_c (GHz)		4,1	8,75	6,85
Pulse parameter a		1,210e9	2,592e9	9,903e9
Maximum amplitude A_{max} (v)	1×1	2,164	4,638	17,718
	2×2	1.531	3.280	12.529
	4×4	1.082	2.319	8.859

The detected frequencies at the target detector are calculated as follows.

$$f = i \cdot \Delta f = i \cdot \frac{f_{s\_bin}}{N_{FFT}} \tag{7}$$

where, i denotes the number of spectral components, Δf denotes the frequency resolution of FFT. f_{s_bin} is the sampling frequency, which is given by

$$f_{s\_bin} = \frac{f_{cg}}{2 \times T_{PN} \times N_{dR} \times N_{decim}} \tag{8}$$

where, Ndecim denotes the performed decimation number. All other parameters of the UWB radar used in the simulations are summarized in Table II.

TABLE II. PARAMETERS USED IN THE SIMULATION

Parameter	**Value**
PRF	1 MHz
ADC quantization	12 bits
Length of PN sequence (N_{PN})	31
weighting window	Hanning/Hamming/Blackman
Number of resolution elements (N_{dR})	128
FFT dimension (N_{FFT})	1024
Decimation number (N_{decim})	6

B. Detection Setting

As shown in Figure 3, the radar is located at the ceiling of a room. In our simulation system, omni antennas are assumed. When 2×2 or 4×4 antenna array are used, the neighbour antennas are separated by a distance of $\lambda/2$, where λ is the wave length at the center frequency of the UWB band. The body skin vibration caused by respiration

and heartbeat is combination of respiration signal *RP(t)* and heartbeat signal *HB(t)*. Suppose that the radar is put in a position right above the subject as shown in Figure 3, the skin vibration caused by respiration and heartbeat will only on Z axis and can be represented as follows.

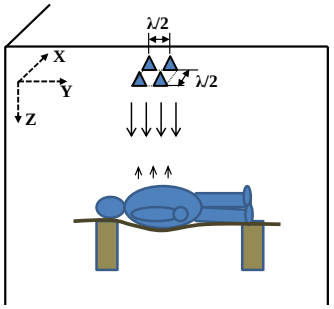

Figure 3. Detection Setting.

$$z(t) = z_0 + A_{RP}\sin(2\pi F_{RP}t + \varphi_{RP}) + A_{HB}\sin(2\pi F_{HB}t + \varphi_{HB}) \quad (9)$$

where, A_{RP} and A_{HB} are the amplitudes, F_{RP} and F_{HB} are the frequencies, φ_{RP} and φ_{HB} are the phases, respectively for respiration and heartbeat signals. Z_0 is the distance between the subject and antenna. The values of amplitudes, frequencies, and phases for respiration and heartbeat used in simulation are summarized in Table III.

We adopt point target model in the simulation. The amount of collected reflected power P_r at the receiver antenna is calculated as

$$P_r = \frac{\sigma G_t G_r \lambda^2 P_t}{(4\pi)^3 r^4} \quad (10)$$

where σ denotes radar cross section. The related reflection area of the target is assigned with values of 20 cm^2 for respiration and 3 cm^2 for heart beat respectively. The antenna gain G_t and G_r are both set to 0 dBi and the transmit power P_t is decided by the allowed UWB power spectrum density (PSD) and bandwidth. The wave length λ is calculated at the center frequency of a given UWB band. Furthermore, thermal noise is assumed with a one-sided power spectral density N_0.

TABLE III. PARAMETERS OF RESPIRATION AND HEARTBEAT.

Parameter	Value
F_{RP}	0.4 Hz
F_{HB}	1.2 Hz
A_{RP}	5mm
A_{HB}	0.5mm
φ_{RP}	0
φ_{HB}	0

IV. SIMULATION RESULTS AND DISCUSSION

In the following, we show some examples of the computer simulation results. Our main concern is put on the examination on the three UWB bands as well as the examination on numbers of antennas. In the developed simulation system, GUI is installed so that one can intuitively observe the detection of a subject. Graphics in both frequency domain and time domain are shown simultaneously through GUI.

Examples of respiration and heartbeat detections on GUI are given in Figures 4 and 5 respectively. In Figure 4, an example of respiration detection using 3.4-4.8 GHz band and with 2×2 antenna array is shown. It can be seen that the respiration frequency is clearly detected at 0.4 Hz, although a small component appears at the two-time harmonic in the

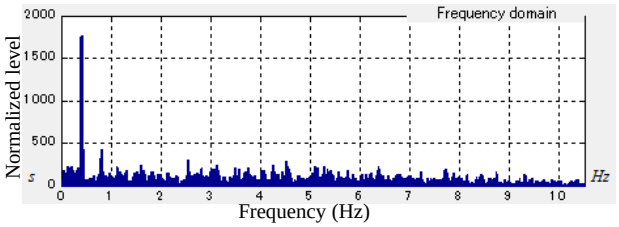

(a) Frequency domain signal

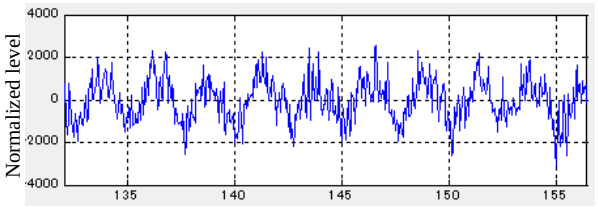

(b) Time domain waveform

Figure 4. Example of respiration detection using 3.4-4.8 GHz.

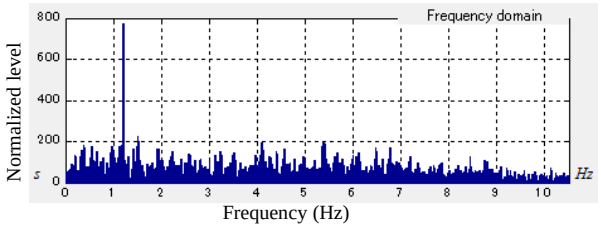

(a) Frequency domain signal

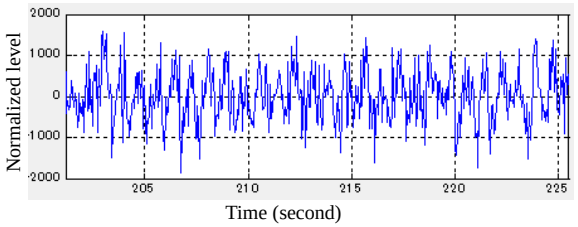

(b) Time domain waveform

Figure 5. Example of heartbeat detection using 7.25-10.25 GHz.

frequency domain. In the time domain, the period of the respiration can be clearly recognized, which is about 2.5s. An example of heartbeat detection using 7.25-10.25 GHz band and with 4×4 antenna array is shown in Figure 5. The heartbeat is detected at 1.2 Hz in frequency domain and the period of heartbeat obtained in time domain is about 0.83s.

In Figure 6, required gains of the VGA that is located after the integrator are obtained. The detection target is respiration and the distance between the subject and radar antenna is fixed at 3m. For comparison convenience, the results are normalized to that of the 1×1 antenna case on 3.1-10.6 GHz band. Evaluation and comparison among the three frequency bands as well as the three patterns of array antennas are made.

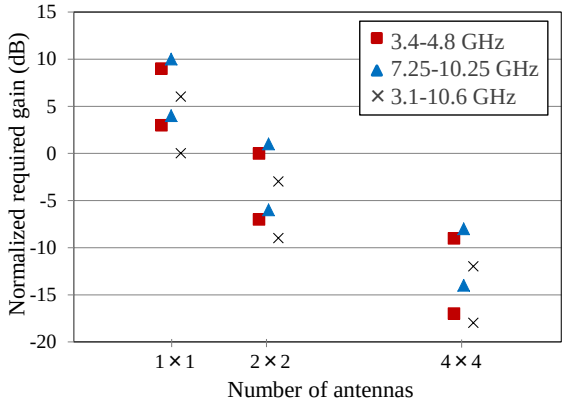

Figure 6. Required gains for respiration detection at a distance of 3m.

It can be seen that for all three frequency bands, increasing the number of antenna can steadily reduce the required VGA gains. Compared to 1×1 antenna, 2×2 array saves 9-10 dB gains, while 4×4 array further saves another 9-10 dB gains compared to 2×2 array. For each case of antenna array, we give two results which correspond to two detection status. The results show that 3.4-4.8 GHz band and 7.25-10.25 GHz band present similar detection ability. In comparison, 3.1-10.6 GHz band can save 3-4 dB gains than the other twos. The reason that 3.4-4.8 GHz band and 7.25-10.25 GHz band give similar results can be explained as follows. On one hand, the center frequency of 3.4-4.8 GHz band is slightly less than half of that of 7.25-10.25 GHz band. On the other hand, 7.25-10.25 GHz band has a slightly larger bandwidth than double that of 3.4-4.8 GHz band. The merit provided by the low center frequency is waived by the merit of large bandwidth.

Next, we investigate the maximum distance for heartbeat detection for the three UWB bands. To make fair comparisons, in each frequency band and for each antenna combination we increase the maximum VGA gains as large as possible until ADC clipping occurs. The obtained results are summarized in Figure 7. It can be seen that when 3.4-4.8 GHz band and 7.25-10.25 GHz band are used, there is not big difference on maximum distance. However, when 3.1-10.6 GHz band is used, the detecting distance is increased. Moreover, increasing the number of antennas results in large detecting distance. In Figure 7, using 3.1-10.6 GHz band with 4 × 4 array, the heartbeat can be detected from a distance of 3.4 m.

Finally, using heartbeat detection as an example, the relation of detecting distance with required gain are depicted in Figure 8. All three UWB band are investigated with 4×4 array and 2×2 array, respectively. The results for 2×2 array are shown with blank symbols while the results for 4×4 are shown with filled symbols. It can be seen that for each combination among the three UWB bands and two types of antenna arrays, the required gain almost linearly increases with detecting distance. The inclinations of increase for all cases are very similar. Except for a single point at 1m, 3.1-10.6 GHz band needs less gain than the other two bands. It is also obvious that 4×4 array presents constant gain against 2×2 array. The gain is around 8-11dB. This number also coincides with the result of respiration detection given in Figure 6, in which the gain obtained by 4×4 array over that of 2×2 array is 9-10 dB. Thus, it is an effective way to increase the radar detectability by increasing antennas.

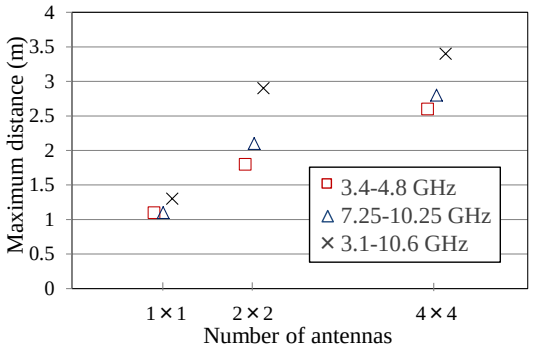

Figure 7. Maximum distance for heartbeat detection

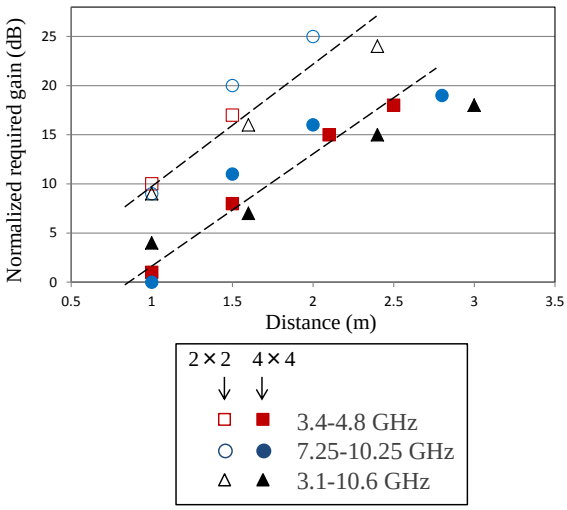

Figure 8. Relation of detecting distance with required gain.

V. CONCLUSION

We conducted preliminary studies on UWB radar with antenna arrays for detection of human respiration and heartbeat. A computer simulation radar system is developed in line with the structure and processing of real radar systems. We also installed a GUI so that the detection of respiration and heartbeat can be shown intuitively.

As our goal is to develop a UWB radar system within the scope of regulation in Japan, the regulated UWB low band, 3.4-4.8 GHz, and UWB high band, 7.25-10.25 GHz, of Japan are investigated. The regulated USA UWB band, 3.1-10.6 GHz is presented as a comparison. Three types of antenna combinations, 1×1, 2×2, and 4×4, are also investigated. The simulation results show that UWB low band and UWB high band of Japan present identical detection performance. Both of them are a little deteriorated by the 3.1-10.6 GHz band. However, if the subject is under rubble, 3.4-4.8 GHz band should be superior because it can go through rubble more easily than the latter. Our results show that increasing antenna is an effective way to enhance detection ability.

REFERENCES

[1] L. Chioukh, H. Boutayeb, L. Lin, L. Yahia, and W. Ke, "Integrated radar systems for precision monitoring of heartbeat and respiratory status", Conference Record, Asia Pacific Microwave Conference 2009 (APMC2009), Singapore, Dec. 2009, pp.405-408.

[2] G. Lu, F. Yang, X. Jing, and J. Wang, "Contact-free measurement of heartbeat signal via a doppler radar using adaptive filtering", Conference Record, 2010 International Conference on Image Analysis and Signal Processing (IASP), Canada, Aug. 2010, pp. 89-92.

[3] O. Postolache, R. N. Madeira, P. S. Girão, and G. Postolache, "Microwave FMCW Doppler radar implementation for in-house pervasive health care system", Conference Record, 2010 IEEE International Workshop on Medical Measurements and Applications Proceedings (MeMeA2010), Canada, may 2010, pp. 47-52.

[4] B. Levitas and J. Matuzas, "UWB radar for breath detection", Conference Record, 11th International Radar Symposium (IRS2010), Lithusnia, June 2010, pp. 1-3.

[5] D. Zito, D. Pepe, M. Mincica, F. Zito, D. De Rossi, A. Lanata, E. P. Scilingo, and A. Tognetti, "Wearable system-on-a-chip UWB radar for contact-less cardiopulmonary monitoring: Present status", Conference Record, 30th Annual International Conference of the IEEE Engineering in Medicine and Biology Society, 2008 (EMBS 2008), Aug. 2008, pp. 5274-5277.

[6] S.-H. Chang, M. Wolf, and J. W. Burdick, "An MHT algorithm for UWB radar-based multiple human target tracking", Conference Record, IEEE International Conference on Ultra-Wideband, 2009 (ICUWB 2009), Canada, Sep. 2009, pp.459-463.

[7] T. Sakamoto and T. Sato, "A target tracking method with a single antenna using time-reversal UWB radar imaging in a multi-path environment", Conference Record, 2010 IEEE International Geoscience and Remote Sensing Symposium (IGARSS2010), Hawaii, July 2010, pp. 3319-3322.

[8] K.-M. Chen, Y. Huang, J. Zhang, A. Norman, "Microwave life-detection systems for searching human subjects under earthquake rubble or behind barrier", IEEE Transaction on Biomedical Engineering, vol.27, no.1 pp.105-114, Jan. 2000.

 ISBN: 978-1-61208-306-3